New Photoiniferters: Respective Role of the Initiating and Persistent Radicals

J. Lalevée,*,† N. Blanchard,‡ M. El-Roz,† X. Allonas,† and J. P. Fouassier†

Department of Photochemistry, UMR 7525 CNRS, University of Haute Alsace, ENSCMu, 3 rue Alfred Werner, 68093 Mulhouse Cedex, France, and Department of Organic and Bioorganic Chemistry, UMR CNRS 7015, University of Haute Alsace, ENSCMu, 3 rue Alfred Werner, 68093 Mulhouse Cedex, France

ABSTRACT: Three new structures (*S*-benzoyl *O*-ethyl xanthate, benzoyl diethyldithiocarbamate, and benzyl 9*H*-carbazole-9-carbodithioate) are proposed as photoiniferters for controlled photopolymerization reactions. They are more efficient than the reference compound—benzyl dimethyldithiocarbamate—for both the polymerization rates of an acrylic difunctional monomer and the final control properties of the MMA photopolymerization (polydispersity PDI = M_w/M_n and/or number-average molecular weight M_n ranges). The best results are obtained with benzyl 9*H*-carbazole-9-carbodithioate (PDI = 1.14 at 10% conversion and 1.5 at 40%; M_n = 16 000 at 20% conversion). Transient radical absorptions were recorded and the interaction rate constants with MMA and oxygen measured by laser flash photolysis. Quantum mechanical calculations show that the singly occupied molecular orbital delocalization is higher for the carbazole derivative. The significant improvement of the control mechanism by benzyl 9*H*-carbazole-9-carbodithioate is due to both the increase of the light absorption of the dormant species and the higher persistent character of the associated radical.

Introduction

Atom transfer radical polymerization (ATRP), reversible addition−fragmentation transfer (RAFT), nitroxide-mediated polymerization (NMP), and the use of iniferters are elegant ways for the development of controlled radical polymerizations (CRP).[1–3] Thermally initiated CRPs are well-known.[1,2] In contrast, the use of light-induced CRP has not received much attention.[1] One interesting way consists of using a photoiniferter capable of behaving as a photoinitiator, a transfer agent, and a control polymerization agent (usually by the generation of a persistent radical, which plays the role of a chain terminator). Recent photopolymer applications include[1,3–8] the synthesis of complex architecture polymers, photografting, manufacture of photomaterials, photolithography, photomodification of polymer, design of new optical materials, change of chemical compatibility or mechanical and adhesion properties, and reinforcement. The systems proposed in the literature,[4–9] although powerful for these applications, lead to a relatively broad M_n distribution.

Very few structures exhibit photoiniferter properties.[6–11] The most popular is benzyl dithiocarbamate (**BDC**)[6–9] which will be used here as a reference since its CRP properties are well-known. We presented asymmetric or symmetric disulfides as new photoiniferters.[10,11] In the present paper, we propose other carefully selected new compounds (Scheme 1) in which both the initiating and the persistent radicals are changed compared to the **BDC** structure. The control properties of these compounds will be examined by the measurements of the polydispersity and the average molecular weights of the formed polymers. Laser flash photolysis and quantum mechanical calculations will elucidate their photochemical behavior.

Experimental Section and Computational Procedure

Photoiniferters and Materials. Benzyl dimethyldithiocarbamate (**BDC**, Aldrich) was used with the best purity available. *S*-Benzoyl *O*-ethylxanthate (**BEX**) and benzoyl diethyldithiocarbamate (**BEC**)

Scheme 1

BDC

BEC

BEX

BCC
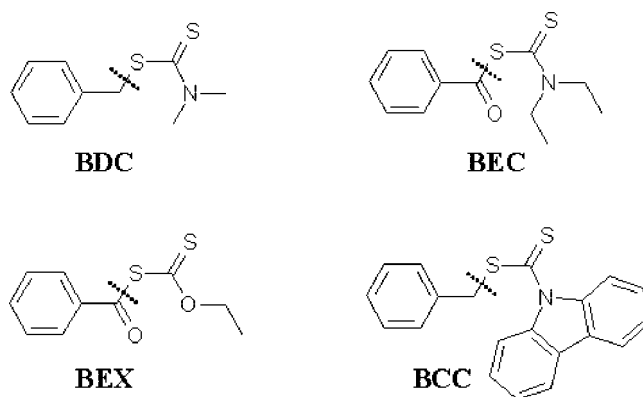
were synthesized by a literature procedure.[12] A similar approach to that presented in ref 13 was used for the synthesis of benzyl 9*H*-carbazole-9-carbodithioate (**BCC**). Full synthesis conditions and characterization (NMR) are given in the Supporting Information.

Methyl methacrylate (MMA), 1,6-hexanediol diacrylate (HDDA), and 2,2′-dimethoxyphenyl acetophenone (DMPA) were used with the best purity available (Aldrich).

Laser Flash Photolysis (LFP) Experiments. The nanosecond laser flash photolysis LFP setup is based on a pulsed Nd:YAG laser (Powerlite 9010, Continuum) and a transient absorption analysis system (LP900, Edinburgh Instruments). The instrument response was equal to about 10 ns.[14]

The benzophenone triplet state (³BP) was used as an actinometer for the determination of the dissociation quantum yields ϕ_{diss} according to eq 1

$$\phi_{diss} = \frac{\Delta OD_S}{\Delta OD_{BP}} \frac{\epsilon_{BP}}{\epsilon_S} \qquad (1)$$

where ΔOD_S, ΔOD_{BP}, ϵ_{BP}, and ϵ_S stand for the optical density change (ΔOD) and the molar extinction coefficients (ϵ) for the sulfur-centered radicals and the triplet state of benzophenone (at λ = 525 nm), respectively. The ΔOD were measured in LFP for the same amount of light absorbed. In eq 1, ϵ_S was calculated by fitting

* Corresponding author. E-mail: j.lalevee@uha.fr.
† UMR 7525 CNRS.
‡ UMR CNRS 7015.

Table 1. Photochemical Properties[a] and Photoinitiating Ability (Relative Rate of Polymerization) of the New Photoiniferters (Scheme 1)

	absorption properties λ in nm (ϵ in M^{-1} cm^{-1})	S_1 energy (kcal/mol)	T_1 energy (kcal/mol)	BDE (kcal/mol)	k_{diss} (s^{-1})	ϕ_{diss}	$R_p{}^b$
BDC	335 (149)	72.1	50.9	31.3	$>10^8$	0.45	1
BEC	405 (52)	67.3	49.6	42.1	$>10^8$	0.17	2
BEX	400 (57)	67.9	54.8	48.6	$>10^8$	0.12	15.7
BCC	365 (5650)	c	42.5	37.7	$>10^8$	0.04	1.5

[a] Maximum absorption wavelength λ, molar extinction coefficient ϵ, singlet S_1 and tiplet T_1 energy, bond dissociation energy BDE, dissociation rate constant k_{diss}, dissociation quantum yield ϕ_{diss}. [b] Relative polymerization rates R_p of a HDDA (1,6-hexanedioldiacrylate); reference: **BDC** (Scheme 1); amount of photoinitiator: 1% w/w. The relative R_p in the presence of a reference UV-photoinitiator (2,2′-dimethoxyphenylacetophenone) is 25 in the same experimental conditions. [c] Not determined: for this large molecule, the calculation time was too long.

the recombination kinetics with a second-order law (rate constant: k_r/ϵ where k_r is the recombination rate constant); k_r was assumed as equal to the diffusion rate constant corrected by the spin multiplicity factor as usually done.[15] For BP, ϵ was extracted from the literature and taken as 6250 M^{-1} cm^{-1}.[15]

Photopolymerization Procedure. The photopolymerization of Ar degassed bulk MMA was carried out in a sealed glass tube (sample thickness: 1 mm) under exposure to the UV light of a Xe−Hg lamp (Hamamatsu, L8252, 200 W). The monomer conversion was directly followed by real-time FTIR spectroscopy (Nicolet, Nexus 870) in the near-infrared spectral region as usually done for thick samples (4700–4800 cm^{-1}).[16] The laminated films of 1,6-hexanediol diacrylate (HDDA) deposited on a BaF_2 pellet (25 mm thick; optical density <0.15 at 366 nm) were irradiated with the same Xe−Hg lamp. The evolution of the double bond content was continuously monitored by real-time FTIR spectroscopy at 1640 cm^{-1}. The rates of polymerization R_p were calculated from the linear part of the % conversion vs time curves as shown in ref 17. The studied compounds were compared to 2,2-dimethoxy-2-phenyl-acetophenone (DMPA), a well-known usual UV photoinitiator.[18]

Molecular Weight Determination. The number-average molecular weights (M_n) and polydispersity index (PDI = M_w/M_n) were determined by gel permeation chromatography GPC using a Waters 2690 apparatus at room temperature equipped with styragel columns (HR0.5, HR1, HR4) and a refractive index detector (Waters 410). The molecular weight resolving range of the columns lies between 500 and 600 000 g mol^{-1}. Polystyrene standards were used in order to generate a universal calibration curve. Tetrahydrofuran (THF) was chosen as an eluant.

Quantum Mechanical Calculations. Molecular orbital calculations were carried out with the Gaussian 03 suite of programs.[19] The C−S bond dissociation energies (BDE) and the triplet energy levels E_T of the investigated structures were calculated with addition of the ZPE correction. The different structures were fully optimized in the density functional theory framework (at the B3LYP/6-31G* level). The relaxed singlet energy levels E_{S_1} were determined with the CIS/6-31G* method. These calculations allow the determination of the dissociation reaction enthalpies either from T_1, $\Delta H_{diss,T_1} = E_T -$ BDE, or from S_1, $\Delta H'_{diss,S_1} = E_{S_1} -$ BDE.

Results and Discussion

Photoinitiating Properties of the Studied Photoiniferters. The photoinitiating properties of the photoiniferter compounds were first investigated in HDDA films (Table 1, Figure 1). The best rate of polymerization (R_p) is obtained for **BEX** and the lowest one for **BDC**. For comparison, the R_p with **BEX** corresponds to about 60% of that of DMPA.

In a classical photopolymerization process involving a cleavable photoinitiator (monomer quenching does not compete), R_p is proportional to the square of the initiation quantum yield ϕ_i given by 2[17]

$$\phi_i = \phi_{diss} k_i[M]/(k_i[M] + k_r) \qquad (2)$$

where k_i and k_r stand for the initiation rate constant and the overall rate constant for the disappearance of the initiating structures through the other processes that compete with the initiation (recombination, hydrogen transfer), respectively.
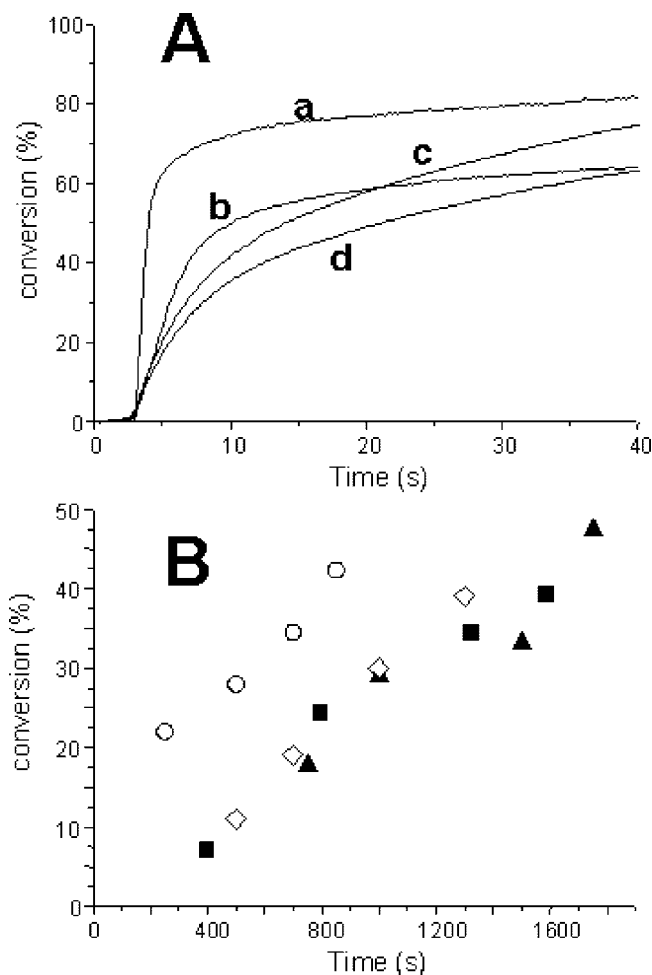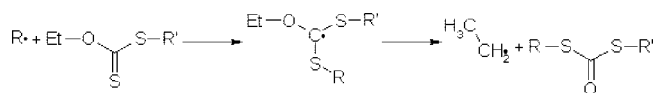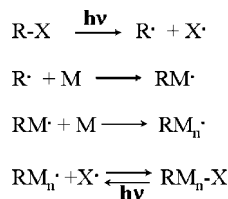

Figure 1. (A) Polymerization profiles for 1,6-hexanediol diacrylate (HDDA). Photoinitiating system (Scheme 1): (a) **BEX**, (b) **BEC**, (c) **BCC**, (d) **BDC** (1% w/w). (B) Polymerization profiles of methyl methacrylate (MMA): (squares) **BDC**; (up triangles) **BEC**; (circles) **BEX**; (diamonds) **BCC**: concentration of 1%, 1%, 1%, and 0.5% (w/w), respectively.

As expected, no correlation between R_p and ϕ_{diss} can be found (Table 1); this indicates that the respective amount of absorbed light as well as the change of k_i must be taken into account in eq 2. Indeed, an important factor is concerned with the initiation ability of the generated carbon-centered radicals: the benzoyl radical is more reactive than the benzyl radical (see below). In **BEX**, the xanthate moiety plays a dramatic role on R_p; it has already been suspected that the Barton−McCombie rearrangement of this moiety can lead to the generation of alkyl radicals (Scheme 2).[20] The high reactivity of these latter species toward the initiation process[21] explains quite well the R_p increase. In **BCC**, the initiating structure is similar to **BDC**. However, its high UV light absorption (see below) ensures a higher efficiency. For **BEX** and **BEC**, the benzoyl radical is an initiating species better than the benzyl radical; therefore, the initiating properties

Scheme 2

Scheme 3

$$R\text{-}X \xrightarrow{h\nu} R\cdot + X\cdot$$

$$R\cdot + M \longrightarrow RM\cdot$$

$$RM\cdot + M \longrightarrow RM_n\cdot$$

$$RM_n\cdot + X\cdot \underset{h\nu}{\overset{}{\rightleftarrows}} RM_n\text{-}X$$

of these compounds are accordingly improved compared to **BDC**.

Controlled Photopolymerization of MMA. The mechanism of a photoiniferter involving CRP is recalled in Scheme 3.[6,7,9–11] The recombination of the persistent radical ($X\cdot$) with the propagating radical is photochemically reversible and gives a living character to the reaction. The exchange between the active $R-Mn\cdot$ and the dormant species $R-Mn-X$ must be fast in comparison with the propagation process. This photodissociation of the polymer chain end and the further propagation repeatedly occurs; as a consequence, the molecular weight will increase with the conversion (the total number of chains is expected to be constant).[1,2] The reference compound **BDC** obeys this mechanism: after the C–S bond cleavage, the benzyl radical $R\cdot$ initiates the polymerization whereas the generated dithiocarbamyl radical $X\cdot$ plays the role of the persistent radical.

The R_ps for the MMA bulk photopolymerization in the presence of the various photoiniferters (Figure 1) exhibit a trend similar to that reported for HDDA: **BEX ≫ BEC, BCC > BDC**. In our experimental conditions, a complete polymerization is achieved in less than 1 h.

The increase of the molecular weight M_n with the conversion as well as the obtained polydispersity PDI represent the best criterions to characterize the control processes.[1–3] Such a behavior demonstrates that the photodissociation of the dormant species, the subsequent propagation associated with the active species, and the recombination with the persistent radical occur. For DMPA, this mechanism obviously does not take place and approximately constant M_n values were found.[11] For all the structures proposed here, the M_n vs conversion plots give linear relationships: the average molecular weight follows a positive linear trend with the conversion as shown in Figure 2. For **BEC**, **BCC**, and **BDC**, the deviation from the origin corresponds to an usual behavior and indicates that a part of the carbon–carbon termination mechanism still remains in the early stages of the reaction, the linear trend being always ascribed to the polymeric radical/persistent radical recombination reaction.[2,9–11] For **BCC**, the M_n values are relatively high (16 000 at 20% conversion).

The PDI values characterize the control mechanism (Figure 3). Using DMPA, no control occurs and large PDIs (up to 5–6) were already noted.[11] The values obtained here for the proposed structures are about 3 times lower with PDIs ranging from 1.7 to 1.8, 1.8–2.1, 1.75–2.5, and 1.1–1.5 for **BDC**, **BEC**, **BEX**, and **BCC**, respectively. For **BEX**, the xanthate conversion (Scheme 2) increases the initiation efficiency and therefore leads to a poorer control.

The PDIs obtained in this photochemical CRP reactions in the presence of **BEX** and **BEC** (and of course **BDC**) can be considered as already interesting compared to the usual PDI values obtained in thermal CRP processes (1.1–1.4).[1,2] For **BCC**, the present results even appear as excellent with a PDI value of 1.14 at 10% conversion and 1.5 at 40%. In addition, the

polymerization times are short (lower than 30 min) compared to those used in thermal polymerization reactions (several hours).

We have also previously demonstrated that a decrease of the light irradiation energy results in a lower instantaneous concentration in the polymeric radicals.[10,11] A better control was consequently obtained since the bimolecular recombination between two propagating radicals was reduced. This procedure applied to **BCC** should be interesting to further increase the control properties if necessary.

Photochemical Properties of the Photoiniferters. The UV–vis absorption properties of the new proposed structures are compared to that of **BDC** in Table 1 and Figure 4. The strongly red-shifted transition noted for **BEC** and **BEX** is ascribed to a n–π* transition associated with the C(O)–S–C(S) chromophore. For **BCC**, a similar shift is also observed. Interestingly, the extinction coefficients are, however, strongly enhanced, thereby indicating a π–π* transition ascribed to the carbazole–C(S)–S moiety. The shifted and/or enhanced absorptions of the new proposed structures are interesting from the point of view of a more efficient light absorption using the near-UV–vis photons of the Hg–Xe lamp. Therefore, a strong enhancement of the dormant species absorption in **BCC** can also be expected through the change of the **BDC** carbamate moiety for the carbazole chromophore. This will be useful for a more efficient reinitiation process under light irradiation (cleavage of the dormant specie as shown in Scheme 3).

The photochemical reactivity of the investigated structures has also been studied through LFP experiments (Table 2). These results are particularly worthwhile since, except for **BEX**,[12] no studies have been reported so far. Just after the laser excitation of the studied compounds at 355 nm, long-lived transient species with lifetimes higher than 50 μs are observed (Figure 5). They are not affected by oxygen ($k_{O_2} < 10^6$ M^{-1} s^{-1}) and are safely ascribed to sulfur-centered radicals as these kinds of species exhibit a weak O_2 sensitivity (Table 2).[22] For **BEX**, the absorption is clearly that of the ethyloxythiocarbonylthiyl radical as previously reported at 650 nm.[12] The transient species observed for **BEC** is assigned to the corresponding dithiocarbamyl radical on the basis of the reported absorption spectrum observed in the case of **BDC** at 600 nm.[10,11] For **BCC**, the absorption maximum located around 600 nm is ascribed to the carbazoledithiocarbamyl radical from similarities with the transient spectra of **BDC** and **BEC**; moreover, a strong bleaching is also noted at λ < 400 nm in agreement with the red-shifted ground-state absorption of **BCC**.

For all the photoiniferters, the rising times of the radical absorption are found within the resolution time of the experimental setup (<10 ns) leading to cleavage rate constants k_{diss} higher than 10^8 M^{-1} s^{-1}. Benzyl (in **BDC**, **BCC**) and benzoyl radicals (in **BEC**, **BEX**) were not observed here as these structures can only be detected at λ < 350 nm.[23] All these results support a very fast C–S single-bond cleavage as depicted in Scheme 1. This cleavage can probably occur in both the S$_1$ and T$_1$ states as supported by quantum calculations carried out on **BDC**.[11] The laser excitation of isopropylthioxanthone ITX ($E_T \sim 63$ kcal/mol) in the presence of the photoiniferters leads to the generation of the sulfur-centered radicals which clearly supports a triplet cleavage (after a triplet–triplet energy transfer from ^{3}ITX). This does not obviously exclude the possibility of a singlet cleavage under direct excitation.

Quantum mechanical calculations were carried out to shed some light on this cleavage process. The C–S bond dissociation energy, the triplet and singlet energy levels, and the dissociation enthalpies ($\Delta H_{diss,T_1}$; $\Delta H_{diss,S_1}$) are important parameters to characterize this process (Table 1). The dissociation quantum yields ϕ_{diss} measured by LFP satisfactorily correlate with both $\Delta H_{diss,T_1}$ and $\Delta H_{diss,S_1}$ (Figure 6), demonstrating that the C–S
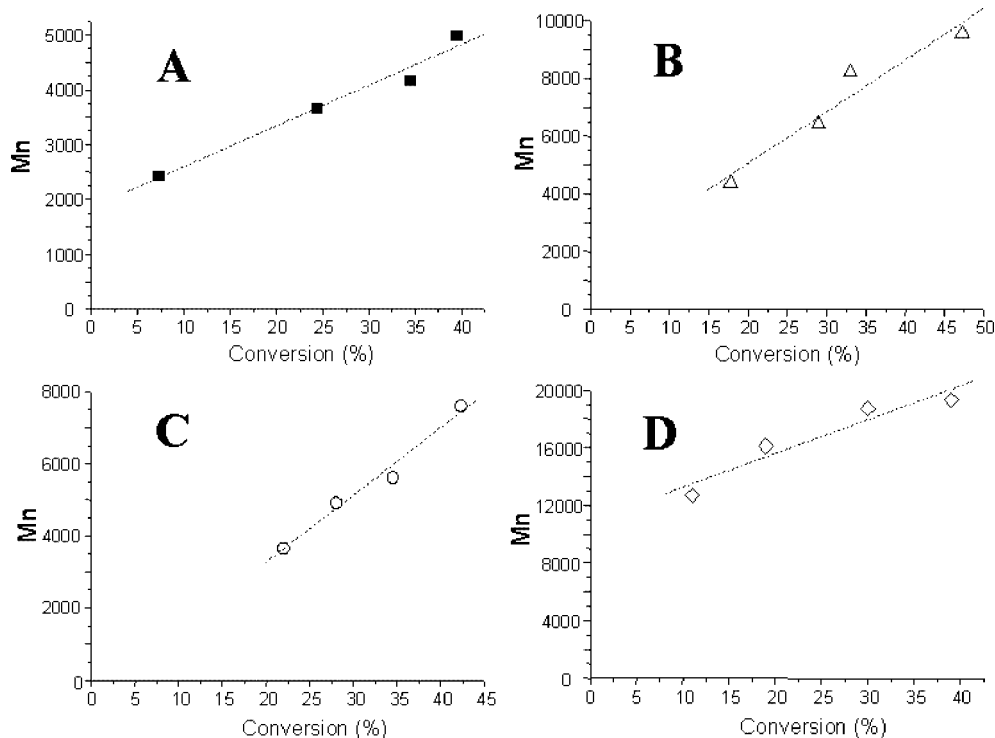
Figure 2. Effect of the photoiniferters (Scheme 1) in the photopolymerization of MMA in bulk: number-average molecular weight M_n vs conversion plots: (A) **BDC**; (B) **BEC**; (C) **BEX**; (D) **BCC**. Photoiniferter concentrations of 1%, 1%, 1%, and 0.5% were used, respectively.
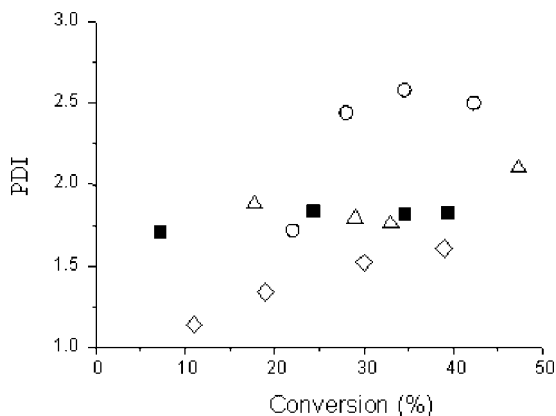

Figure 3. Effect of the photoiniferters (Scheme 1): PDIs vs conversion plots. MMA in bulk. **BDC** (squares); **BEC** (up triangles); **BEX** (circles); **BCC** (diamonds).

Figure 4. Absorption spectra of the photoiniferters in acetonitrile for **BDC** (a), **BEC** (b), **BEX**, (c) and **BCC** (d) (Scheme 1).

bond cleavage is probably governed by the reaction enthalpy. From these results, the triplet and singlet cleavage can also be expected. This should be useful for the design of new molecules exhibiting higher ϕ_{diss}.

The reactivity of the generated sulfur-centered radicals toward the addition process to methyl methacrylate MMA was also investigated (Table 2). The lifetime is found unaffected even for [MMA] = 3 M. This leads to an upper limit value for the initiation rate constant k_i about 10^3 M^{-1} s^{-1}, indicating a persistent character. The generated benzyl and benzoyl radicals are more efficient initiating structures for the addition to acrylate or methacrylate units (for example, the addition rate constants are 4.3×10^2 and 2.7×10^5 M^{-1} s^{-1} for methyl acrylate, respectively).[22,23]

The significant improvement of the control mechanism gained by the introduction of the carbazole group in **BCC** can be ascribed to (i) the increase of the light absorption of the dormant species leading to a more efficient cleavage process and (ii) the higher persistent character of the associated radical. For sulfur-
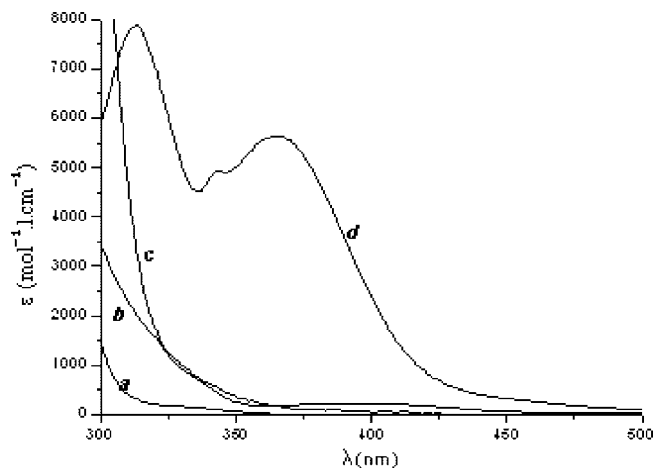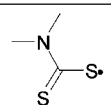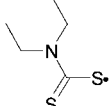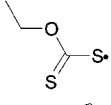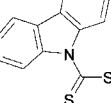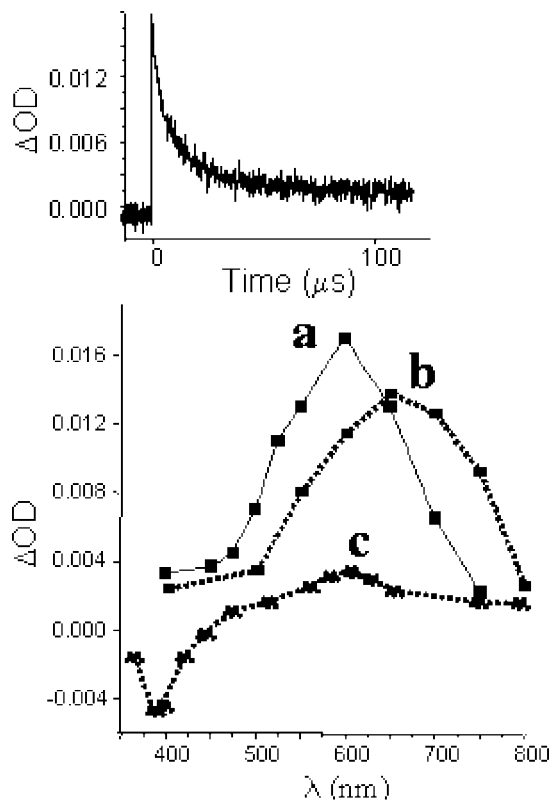
based iniferters, it is well-known that some side reactions of the thiyl radicals (recombination, double bond addition, etc.)[9] lead to a poorer control than that observed with other persistent radicals (for example, the nitroxide radical in the NMP process).[1,2] The more stabilized sulfur-centered controlling agent of **BCC** can be useful to overcome this limitation. In fact, the reactivity of the carbazole-derived radicals (Table 2) is much lower toward the recombination with 2,2,6,6-tetramethylpip-eridine-*N*-oxyl radical (TEMPO) compared to the other car-bamoyl- or xanthate-derived radicals. For **BCC**, the spin population on the sulfur atom is the lowest (Table 2), in agreement with the associated lower reactivity. This is also exemplified by the shapes of the singly occupied molecular orbital (SOMO) of the different structures (Figure 7): the SOMO delocalization is higher for the carbazole derivative **BCC** than for the diethyldithiocarbamyl moiety derivative **BEC**. Interest-ingly, for the thiyl radicals, the final control ability decreases with an increase of the spin population on S (and therefore with

**Table 2. Reactivity of the Different Radical Control Agents:
Addition Rate Constants to Various Additives and Spin Density
on the Sulfur Atom[a]**

	k (M⁻¹s⁻¹) O₂	k (M⁻¹s⁻¹) MMA	k (M⁻¹s⁻¹) TEMPO
	$<10^5$	$<10^3$	$5.5\ 10^7\ (0.522^a)$
	$<10^5$	$<10^3$	$6.5\ 10^7\ (0.523^a)$
	$<10^5$	$<10^3$	$1.0\ 10^9\ (0.589^a)$
	$<10^3$	$<10^3$	$<1.1\ 10^5\ (0.511^a)$

[a] Spin density on the sulfur atom calculated at the UB3LYP/6-31G*
level.

Figure 6. Plots of ϕ_{diss} vs $\Delta H_{diss,T_1}$ (squares) and ϕ_{diss} vs $\Delta H_{diss,S_1}$ (circles). See text.

Figure 5. Transient absorption spectra (at $t = 0$ μs) observed upon
laser excitation of (a) **BEC**; (b) **BEX**; (c) **BCC** at 355 nm in acetonitrile
(Scheme 1). Inset: transient decay for **BEC** at 600 nm.
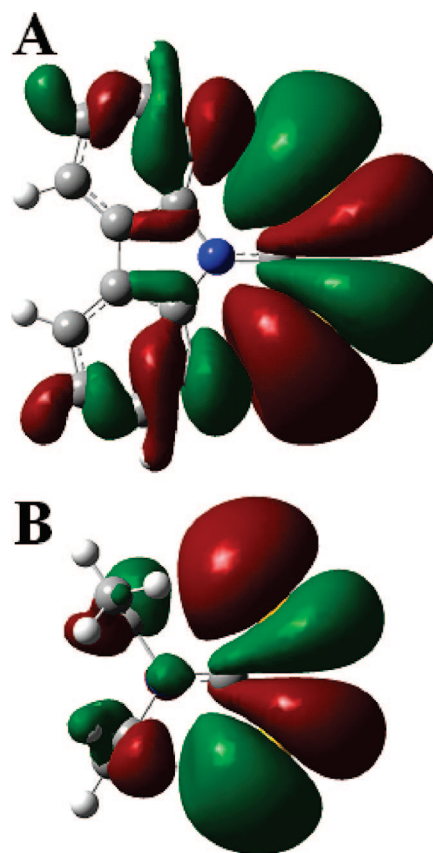
Figure 7. SOMOs of the sulfur-centered radicals derived from **BCC**
(A) and **BEC** (B).

an increase of the reactivity) in the series **BEX** > **BDC**, **BEC**
> **BCC**.

Conclusion

In this paper, for photoiniferters the respective role of the
initiating and persistent radicals are examined. The change from
the benzyl to the benzoyl moieties in a **BDC**-type structure leads
to a drastic enhancement of R_p without any strong disadvanta-
geous effects on the polymerization control. The introduction

of a new carbazole chromophore into the dithiocarbamate moiety
in **BCC** clearly leads to a better control process. To the best of
our knowledge, the obtained PDIs represent the narrower values
never reported so far when using photoiniferters. Highly
stabilized sulfur-centered radicals that do not exhibit side
reactions are found as better persistent species. The highly
efficient character of **BCC** clearly opens up new opportunities
for the synthesis of well-controlled complex polymer architec-
tures through a photochemical approach. As **BCC** was also
recently reported as an efficient RAFT agent for thermal
processes,[13] the combination of a RAFT/photoiniferter procedure
as a dual thermal/photochemical CRP process deserves to be
studied in a forthcoming paper.

Supporting Information Available: ^{1}H and ^{13}C NMR spectra of **BCC** (Figure 1) and the full synthesis. This material is available free of charge via the Internet at http://pubs.acs.org.

References and Notes

(1) (a) Matyjaszewski, K. In *Advances in Controlled/Living Radical Polymerization*; ACS Symposium Series; American Chemical Society: Washington, DC, 2002. (b) Matyjaszewski, K. In *Controlled Radical Polymerization*; ACS Symposium Series; American Chemical Society: Washington, DC, 1998.

(2) Otsu, T. *J. Polym. Sci., Part A: Polym. Chem.* **2000**, *38*, 2121–2136.

(3) (a) Reddy, S. K.; Sebra, R. P.; Anseth, K. S.; Bowman, C. N. *J. Polym. Sci., Part A.: Polym. Chem.* **2005**, *43*, 2134–2144. (b) Luo, N.; Metters, A. T.; Hutchinson, J. B.; Bowman, C. N.; Anseth, K. S. *Macromolecules* **2003**, *36*, 6739–6745.

(4) (a) Otsu, T.; Matsunaga, T.; Doi, T.; Matsumoto, A. *Eur. Polym. J.* **1995**, *31*, 67–78. (b) Otsu, T.; Yamashita, K.; Tsuda, K. *Macromolecules* **1986**, *19*, 287–290.

(5) Otsu, T.; Yoshida, M.; Tazaki, T. *Makromol. Chem., Rapid Commun.* **1982**, *3*, 133–140.

(6) Otsu, T.; Yoshida, M. *Makromol. Chem., Rapid Commun.* **1982**, *3*, 127–132.

(7) Kuriyama, A.; Otsu, T. *Polym. J.* **1984**, *16*, 511–514.

(8) Otsu, T.; Taraki, T. *Polym. Bull.* **1986**, *16*, 277–284.

(9) Bertin, D.; Boutevin, B.; Gramain, P.; Fabre, J. M.; Montginoul, C. *Eur. Polym. J.* **1998**, *34*, 85–90.

(10) Lalevée, J.; Allonas, X.; Fouassier, J. P. *Macromolecules* **2006**, *39*, 8216–8218.

(11) Lalevée, J.; El-Roz, M.; Allonas, X.; Fouassier, J. P. *J. Polym. Sci., Part A: Polym. Chem.* **2007**, *45*, 2436–2442.

(12) Ajayaghosh, A.; Das, S.; George, M. V. *J. Polym. Sci., Part A: Polym. Chem.* **1993**, *31*, 653–659.

(13) Hua, D.; Zhang, J.; Bai, R.; Lu, W.; Pan, C. *Macromol. Chem. Phys.* **2004**, *205*, 1125–1130.

(14) Lalevée, J.; Allonas, X.; Fouassier, J. P. *J. Am. Chem. Soc.* **2002**, *124*, 9613–9621.

(15) (a) Murov, S. L.; Carmichael, I.; Hug, G. L. *Handbook of Photochemistry*; Marcel Dekker: New York, 1993. (b) Alam, M. M.; Watanabe, A.; Ito, O. *Photochem. Photobiol.* **1996**, *63*, 53–59.

(16) Stansbury, J. W.; Dickens, S. H. *Dent. Mater.* **2001**, *17*, 71–79.

(17) Lalevée, J.; Allonas, X.; Jradi, S.; Fouassier, J. P. *Macromolecules* **2006**, *39*, 1872–1879.

(18) Fouassier, J. P. *Photoinitiation Photopolymerization and Photocuring*; Hanser Publishers: Munich, 1995.

(19) (a) Frisch M. J.; Trucks, G. W.; Schlegel, H. B.; Scuseria, G. E.; Robb, M. A; Cheeseman, J. R; Zakrzewski, V. G.; Montgomery, J. A., Jr.; Stratmann, R. E.; Burant, J. C.; Dapprich, S.; Millam, S.,; Daniels, A. D; Kudin, K. N.; Strain, M. C.; Farkas, O.; Tomasi, J.; Barone, V.; Cossi, M.; Cammi, R.; Mennucci, B.; Pomelli, C.; Adamo, C.; Clifford, S.; Ochterski, J.; Petersson, G. A.; Ayala, P. Y.; Cui, Q.; Morokuma, K.; Salvador, P.; Dannenberg, J. J. ; Malick, D. K.; Rabuck A. D.; Raghavachari, K.; Foresman, J. B.; Cioslowski, J.; Ortiz, J. V.; Baboul, A. G.; Stefanov, B. B.; Liu, G.; Liashenko, A.; Piskorz, P.; Komaromi, I.; Gomperts, R.; Martin, R. L.; Fox, D. J.; Keith, T.; Al-Laham, M. A.; Peng, C. Y.; Nanayakkara, A.; Challacombe, M.; Gill, P. M. W.; Johnson, B.; Chen, W.; Wong, M. W.; Andres, J. L.; Gonzalez, C.; Head-Gordon, M.; Replogle, E. S.; Pople, J. A. *Gaussian 98*, revision A.11; Gaussian, Inc.: Pittsburgh, PA, 2001. (b) Foresman J. B.; Frisch A. In *Exploring Chemistry with Electronic Structure Methods*, 2nd ed.; Gaussian Inc.: Pittsburgh, PA, 1996.

(20) Zard, S. *Radical Reactions in Organic Synthesis*; Oxford University Press: New York, 2003.

(21) Fischer, H.; Radom, L. *Angew. Chem., Int. Ed.* **2001**, *40*, 1340–1371.

(22) (a) Colley, C. S.; Grills, D. C.; Besley, N. A.; Jockusch, S.; Matousek, P.; Parker, A. W.; Towrie, M.; Turro, N. J.; Gill, P. M. W.; George, M. W. *J. Am. Chem. Soc.* **2002**, *124*, 14952–14958. (b) Lalevée, J.; Allonas, X.; Morlet-Savary, F.; Fouassier, J. P. *J. Phys. Chem. A* **2006**, *110*, 11605–11612.

(23) Lalevée, J.; Allonas, X.; Fouassier, J. P. *J. Phys. Chem. A* **2004**, *108*, 4326–4334.

MA702406B